Bull. Mater. Sci., Vol. 7, Nos 3 & 4, October 1985, pp. 253–270. © Printed in India.

Magnetic, Mössbauer and electrical properties of Ti-substituted $Ni_{0.3}Zn_{0.7}Fe_2O_4$

D C KHAN and M MISRA*

Department of Physics, Indian Institute of Technology, Kanpur 208016, India

*Present address: Department of Physics, Christ Church College, Kanpur 208001, India

Abstract. The effect of addition of Ti^{4+} in small amounts (1/2, 1, 2, 5, 10% by weight of TiO_2) under oxidising conditions on magnetisation, Mössbauer spectra and resistivity of $Ni_{0.3}Zn_{0.7}Fe_2O_4$ is studied. Analysis of the magnetic data on the basis of 3 sublattice Yafet-Kittel model gives the transfer rate of Fe^{3+} ions between the *A* and *B* sublattices, the distribution of Ti^{4+} and vacancies between them and the five exchange constants of Ni-Zn ferrite. The observed Mössbauer spectra at room temperature are quadrupole doublets and those at liquid nitrogen temperature are magnetic sextets with large relaxation effects. The resistivity shows an increase by about two orders of magnitude due to Ti^{4+} addition.

1. Introduction

The aim of the present work has been to study the effect of addition of Ti^{4+} in small amounts on the magnetisation, Mössbauer and resistivity of Ni-Zn ferrite when the introduction of Ti^{4+} is made under oxidising atmosphere, resulting in the creation of vacancies. The concentration of zinc ($x = 0.7$) in $Ni_{1-x}Zn_xFe_2O_4$ was chosen in the range $x > 0.5$ as this range is physically more interesting due to presence of canting in the *B*-sublattice (Satya Murthy *et al* 1969). The saturation magnetisation showed a variation with Ti^{4+} concentration with a minimum at 1%. The results were analysed on the basis of a three sublattice Yafet-Kittel model, leading to information on the distribution of Ti^{4+} and Fe^{3+} in the sublattices and the values of the five exchange constants.

The motivation of the present work is to look into the effect of localised charge modifications in ferrites on the Fe^{3+} transfer between *A* and *B* sites and on the *BB* interaction. Ti^{4+} is chosen as the agent of this modification since its magnetic moment is zero in its free ionic state and its valency is different from those of the cations of the system. Ni-Zn ferrite of general composition $Ni_{1-x}Zn_xFe_2O_4$ ($x = 0.0$ to 1.0) have been extensively studied (Boxer *et al* 1965), specially with respect to the properties related to the magnetic structure. Normally Ni^{2+} occupies the octahedral (*B*) position, Zn^{2+} occupies the tetrahedral (*A*) position and Fe^{3+} is distributed between the tetrahedral and octahedral sites. For increasing Zn concentration the Fe^{3+} ions at the *A* site decrease while Fe^{3+} at the *B* site increase, causing the total magnetic moment to increase. However, for $x > 0.5$ the *BB* interaction becomes stronger and a noncollinear Yafet-Kittel type magnetic ordering sets in the *B*-sublattice. The Yafet-Kittel angles are

* This paper is dedicated to the memory of the late Dr N S Satya Murthy.

found to increase with increasing Zn^{2+} concentration, resulting in a decrease of the net moment.

If one starts with the Ni-Zn ferrite of a given concentration ($Ni_{0.3}Zn_{0.7}Fe_2O_4$ for our case) and introduces a nonmagnetic ion of higher valency (e.g. Ti^{4+}), the requirement of charge balance will initiate Fe^{3+} transfer through two different kinds of processes depending on the oxygen atmosphere. The replacement mechanism in the reducing atmosphere will be

$$2Fe^{3+} \rightarrow Ti^{4+} + Fe^{2+};$$

since Fe^{3+} cannot be reduced to Fe^{2+}, the charge balance requirement of Ti^{4+} amongst di- and trivalent cations will generate vacancies at both *A* and *B* sites, if the Ni : Zn : Fe contents are kept constant during the preparation.

The representative work which was done earlier was that in Mn-Zn ferrite where $2Fe^{3+}$ are replaced by $Ti^{4+} + Fe^{2+}$ ions in octahedral sites (Stijntjes *et al* 1970). In Ni-ferrite the partial substitution of Fe^{3+} by Ti^{4+} is possible in tetrahedral positions and in $NiZn_{0.5}FeTi_{0.5}O_4$ the possibility of Ti^{4+} replacing Fe^{3+} ions is greater in *B* sites (Gorter 1954). The effect of Ti^{4+} substitution in Fe_3O_4 is studied by Bongers *et al* (1968), concluding that there is no characteristic site preference for Ti^{4+}. Theories of Dunitz and Orgel (1957) and McClure (1957) which are based on crystal field theories using pure ionic type bonding and the theory of Blasse (1964) who assumed the bonds between the metal ion and the oxygen ion to be covalent, are not properly usable in our case since Ti^{4+} does not have a *d*-electron. So the Ti^{4+} occupancy for the present system was determined from the present data without any bias derived from any previous theoretical work. The analysis yielded also the Yafet-Kittel angles at different Ti^{4+} concentrations.

2. Preparation of samples

Analytical reagent grade Fe_2O_3, ZnO, $NiCO_3 \cdot 2Ni(OH)_2 \cdot 4H_2O$ and laboratory reagent grade TiO_2 powders were used. A large quantity of the properly mixed powder for the base composition corresponding to the product ($Ni_{0.3}Zn_{0.7}Fe_2O_4$) was first prepared. Two inch diameter pellets of this composition were calcined at 650°C for 1·5 hours, then dry mixed for 2·5 hours in a high alumina porcelain pot. They were pelletized again and ferritized at 900°C for 5 hours. TiO_2 was added to the ferritized material on the basis of weight percentages and different batches were subjected to wet grinding for about 33 hours and the slurries dried in the oven. The dried powder was mixed with polyvinyl alcohol and moisture and was pressed into 1·29 cm diameter pellets. Sintering was done in a furnace at 1250°C for 20 hours by covering the material to be sintered completely with packing powder and maintaining proper oxygen pressure to prevent expulsion of zinc. The packing material had the same zinc content as the sample, which provided suffcient oxygen pressure for the reaction to take place under oxidizing atmosphere, leading to creation of vacancies when Ti^{4+} enters the system (Ni : Zn : Fe contents being kept constant).

X-ray data on ferritized material were compared with the available ASTM data on $Ni_{0.5}Zn_{0.5}Fe_2O_4$ (ASTM powder diffraction file no. 8-234). With the exception of two lines at *d*-spacings 1·41 Å and 1·17 Å, all the lines of the ASTM file were at least partially

developed at 900°C and fully at 1250°C. Hence ferritization was almost complete at 900°C and definitely at 1250°C.

3. Experimental

The high temperature magnetisation measurements were done on a model 150A vibrating sample magnetometer with a model 151 high temperature oven attachment, supplied by M/s Princeton Applied Research Corporation, USA. The measurements of magnetisation between liquid nitrogen and room temperature were made on a Sucksmith ring balance.

The Mössbauer spectra were recorded with a constant acceleration spectrometer (Encardiorite, India) and a Nuclear Data (USA) ND-60 multi-channel analyser. ^{57}Co embedded in an Rh matrix source supplied by Radio-chemical Centre, Harwell was used. Approximately 30 mg/cm^2 of properly powdered material was used both at room temperature and at liquid nitrogen temperature. Calibration of the spectra was done with natural iron and some times with enriched iron standard sample.

The resistivity from room temperature upto 250°C was measured by the four pin method. The temperature of the sample was varied by placing the probe assembly in a small oven. The samples used were thin rectangular platelets of dimension 4 mm × 9 mm × 0·5 mm. A non-conducting boundary is produced by keeping the sample in contact with mica-sheet.

3.1 *Magnetisation measurements*

We found that at 6 kilo Gauss field the samples are completely saturated and around this field the slow rise of magnetisation is due to the field dependence of intrinsic magnetisation.

Saturation magnetisation was obtained by the extrapolation of the magnetisation vs temperature curve (figure 1) through liquid nitrogen temperature to 0°K. The closed circles in figure 2 show magnetic moment per formula unit in Bohr magnetons at different Ti^{4+} concentrations. A brief report of these results were presented at the 27 Annual MMM Conference at Atlanta, USA, in 1981 (Khan *et al* 1982).

These results were analyzed by using the three sublattice Yafet-Kittel type model of Satya Murthy *et al* (1969) in which the magnetic moments in the sublattices B_1 and B_2 are oriented at an angle $(\pi\text{-}\phi)$ in opposite directions with respect to the moments in the A-sublattice (appendix).

Figure 2 compares the experimental and calculated magnetic moments. This analysis suggests that all Ti^{4+} is going to the A site accompanied by half its number of vacancies for 1/2 to 1%, and starts entering B sites beyond that. The Fe^{3+} transfer is always from A to B sites. The transfer increases from 1/2 through 2% samples and then decreases and reaches approximately a steady state at 5 and 10% systems. The detailed cation distributions are given in table 1.

As is seen from figure 2, this analysis does not exactly account for the sudden steep fall of the moment at 1/2% TiO_2 addition but produces the overall characteristic shape of the moment variation curve. Similar variation of moment has been observed for other systems, i.e. Sn^{4+} and Zr^{4+} addition in $Ni_{0.3}Zn_{0.7}Fe_2O_4$ under oxidizing conditions but these data are available only at room temperature (Das *et al* 1985). The

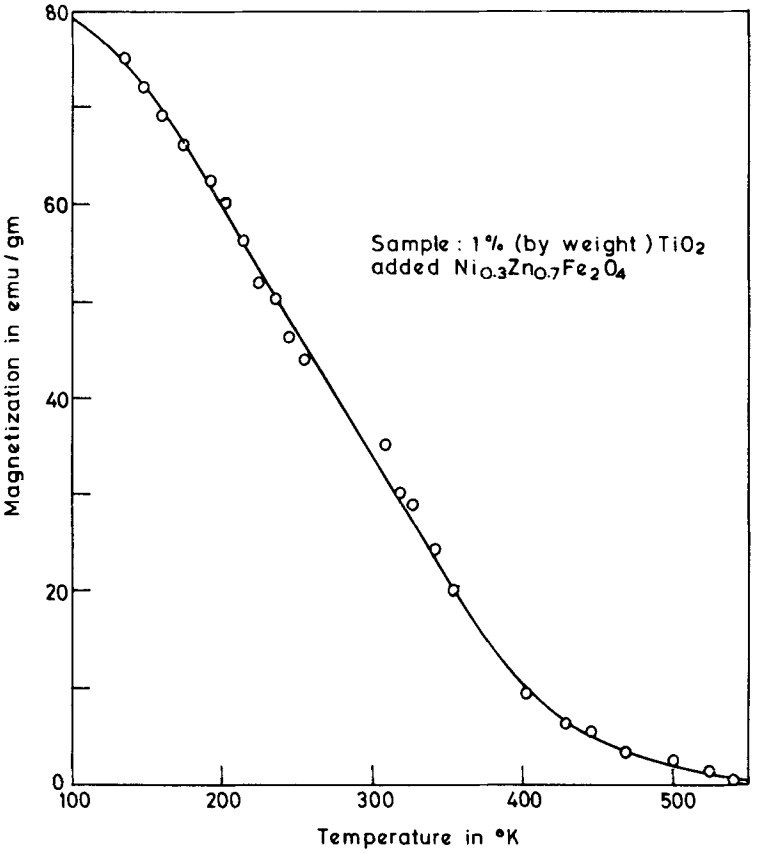

Figure 1. Variation of saturation magnetization with temperature for 1% TiO_2 addition to $Ni_{0.3}Zn_{0.7}Fe_2O_4$ (by Sucksmith ring balance).

lack of sufficient data on similar vacancy introduced systems like ours restricts us from assigning any special magnetic behaviour to vacancies and Ti^{4+} ions. The only thing that can be stated with confidence is that the sudden fall in moment for all small percentages of these additives is too large to be accounted for completely by the molecular field theory in any simple manner.

A very important outcome of the present analysis is that it results in the determination of the constants for all the microscopic exchange interactions of the system. The results are compared with those of Srivastava *et al* (1979) in table 2. Considering the fact that the results in the two cases were deduced from different kinds of measurements on different systems, the agreement could be considered quite satisfactory.

3.2 *Mössbauer measurements*

The Mössbauer spectra of $Ni_{1-x}Zn_xFe_2O_4$ has been extensively studied (Goldanskii and Belov 1965, 1966; Satya Murthy *et al* 1969; Daniels and Rosencwaig 1970; Raj and Kulshresta 1971; Leung *et al* 1973). Daniels and Rosencwaig (1970) found that at room temperature the Mössbauer spectra of $Ni_{1-x}Zn_xFe_2O_4$ series (from $x = 0{\cdot}00$ to $0{\cdot}40$)

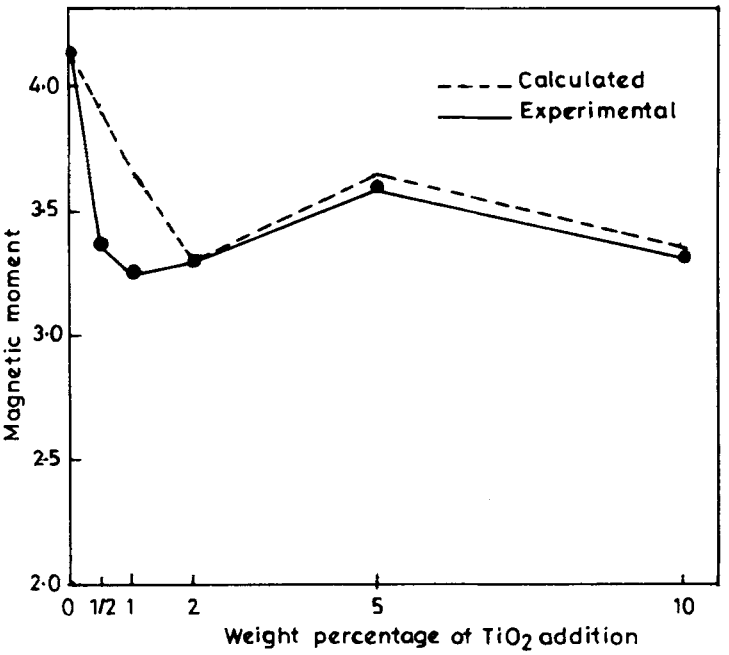

Figure 2. Variation of magnetic moment with addition of Ti in $Ni_{0.3}Zn_{0.7}Fe_2O_4$.

Table 1. Ionic distribution for different TiO_2 concentrations in $Ni_{0.3}Zn_{0.7}Fe_2O_4$

TiO_2 addition in weight percent	Molecular formula unit ( ) *A* sublattice, *B* sublattice, vacancies
1/2	$(Zn_{0.695}Fe_{0.283}Ti_{0.015}\square_{0.007})$ $[Ni_{0.298}Fe_{1.702}]O_4$
1	$(Zn_{0.689}Fe_{0.266}Ti_{0.030}\square_{0.015})$ $[Ni_{0.295}Fe_{1.705}]O_4$
2	$(Zn_{0.679}Fe_{0.239}Ti_{0.054}\square_{0.027})$ $[Ni_{0.291}Fe_{1.701}Ti_{0.005}\square_{0.003}]O_4$
5	$(Zn_{0.649}Fe_{0.263}Ti_{0.058}\square_{0.029})$ $[Ni_{0.278}Fe_{1.590}Ti_{0.088}\square_{0.044}]O_4$
10	$(Zn_{0.600}Fe_{0.243}Ti_{0.105}\square_{0.052})$ $[Ni_{0.257}Fe_{1.472}Ti_{0.180}\square_{0.090}]O_4$

Table 2. J_{AB} exchange constants of Ni-Zn-ferrite

Fe_A^{3+}-Ni_B^{2+}	Fe_A^{3+}-Fe_B^{3+}	Ni_B^{2+}-Ni_B^{2+}	Fe_B^{3+}-Ni_B^{2+}	Fe_B^{3+}-Fe_B^{3+}	References
−23·0	−23·3	+22·0	−4·2	−6·7	Present work
−27·4	−30·7	+30·0	−2·7	−5·4	Srivastava *et al* (1979)

exhibit a well-defined spectrum consisting of two separate six-line Zeeman patterns, due to Fe^{3+} ions at *A* and *B* sites. For $x = 0{\cdot}62$ the spectrum is a relaxed one whereas for $x \geqslant 0{\cdot}70$ the spectra are very similar to paramagnetic spectrum with an intense octahedral doublet and a weak tetrahedral singlet. The zero quadrupole shift of the

magnetic spectra is accounted for by the chemical disorder introduced by the presence of vacancies and non-magnetic ions distributed around Fe^{3+} ions at the B site.

Raj and Kulshrestha (1971) studied $Ni_{1-x}Zn_xFe_2O_4$ series for $x = 0{\cdot}5$ and $x = 0{\cdot}75$ at different temperatures and attempted an explanation of the observed relaxed magnetic spectrum by assuming the existence of collective spin flipping as in the case of superparamagnetic relaxation. However, later neutron diffraction (Bongers *et al* 1968), Mössbauer (Daniels and Rosencwaig 1970; Leung *et al* 1973) and FMR studies (Srivastava and Patni 1970) discarded the hypothesis of the existence of paramagnetic clusters.

Srivastava *et al* (1976) showed that in the $Zn_xFe_{3-x}O_4$ system (for $x > 0{\cdot}2$), Mössbauer spectra have distinct relaxation effects as do Ni-Zn ferrite. They interpreted the relaxation effects in the line shape as being due to domain wall displacements.

Since our spectra also reveal extensive relaxation effects, we briefly discuss the cause and effects of relaxation before presenting our results.

3.3 *Relaxation effects*

The environment of the Mössbauer nucleus may rapidly change due to (i) time-dependent magnetic interaction arising out of electronic spin-spin or spin-lattice relaxation, (ii) randomly changing electric quadrupole interaction due to Jahn-Teller distortion and (iii) interstitial or vacancy diffusion in the vicinity of the nucleus. The line shapes may be quite unusual because of the fluctuating Hamiltonian.

Let the fluctuating magnetic field jump at random between two values $+H$ and $-H$ along the Z-axis and also a symmetric electric field gradient exist along the Z direction. The Mössbauer spectrum displays full Zeeman splitting with slight line broadening when the jump rate is very slow (Blume and Tjon 1968). In this case the photon from the excited nucleus in the magnetic field is emitted before the nucleus sees the changed magnetic field $-H$. Again, when the jump rate is very rapid, the nuclear spin can scarcely precess before it finds that the ionic spin has made a transition and it is in a field $-H$. The limiting time averaged field $\bar{H} = 0$. The Mössbauer spectrum will be a singlet or a doublet. For intermediate jump rates, it has been shown (Blume and Tjon 1968) that the spectrum collapses when the transition probability between the states $+H$ and $-H$ are

$$W = (g_0 m_0 - g_1 m_1)\mu_N H \tag{1}$$

where g and m are the Lande's splitting factor and the magnetic quantum number of the nuclear state, and 0 and 1 represent the ground and the excited state respectively. This condition is satisfied for different values of W for each pair of lines in the sextet. The inner pair will collapse into their center of gravity for values of W smaller than the outer pair. Hence as the jump rate increases, the inner pair first start converging and eventually the outer pair. Thus considerable variety of behaviour can be seen as the jump rate increases.

4. Results and discussion

Here we report the Mössbauer studies made on polycrystalline $Ni_{0{\cdot}3}Zn_{0{\cdot}7}Fe_2O_4$ and with TiO_2 addition samples at room temperature and at liquid nitrogen temperature.

Figures 3 to 5 give the observed Mössbauer spectra. The Mössbauer spectrum for pure $Ni_{0.3}Zn_{0.7}Fe_2O_4$ at room temperature is a relaxed magnetic six peak Zeeman pattern with large line widths. This is due to the fact that the Zeeman pattern for Fe^{3+} at *A* and *B* sites have overlapped because of the relaxation effect. This relaxation is not due to critical fluctuation near T_c as T_c is about 160°C higher than room temperature. As soon as Ti^{4+} ions go into the system (under the oxidising conditions resulting in creation of vacancies), the Mössbauer spectrum at room temperature becomes a paramagnetic spectrum giving only quadrupole splitting. Attempts were made to fit the data with a doublet for the *B* site and a singlet for the *A* site. But the singlet intensity appears to be negligibly small compared to that of the doublet. This led us to conclude that the *A* site environment has also developed a distortion causing a non-cubic symmetry. Also we note that the T_c's of the samples with different concentrations are about 90°C lower than the zero concentration sample. Hence the room temperature data are closer to the T_c, giving a reason why the magnetic peaks should weaken. However, the fact that it completely disappears leads to the conclusion that the relaxation frequency is much larger than the Zeeman frequency.

Figures 6 and 7 give the Mössbauer spectra obtained at liquid nitrogen temperature. For a pure $Ni_{0.3}Zn_{0.7}Fe_2O_4$ sample the relaxation effect has decreased at this temperature as all peaks are of practically the same height with the inner two peaks slightly larger than the other. Still the relaxation effects are large and there is an asymmetry in the width of the peaks; the peaks on one side of the centre are narrower than the peaks on the other side.

For a $Ni_{0.3}Zn_{0.7}Fe_2O_4$ sample with 1/2 TiO_2 added the Mössbauer spectra is a typical relaxed spectra where the inner peaks are of larger intensity than the outer peaks. Here again the inner peaks show some asymmetry.

In the Mössbauer spectrum of $Ni_{0.3}Zn_{0.7}Fe_2O_4$ sample with 1% TiO_2 added, the relaxation has become more intense resulting in the growth of the inner peaks and decrease of outer peaks. Because of broadening or due to some other relaxation effect the inner two peaks have merged into one. In the Mössbauer spectrum of $Ni_{0.3}Zn_{0.7}Fe_2O_4$ with 2% TiO_2 added the effect of the relaxation phenomenon is less but instead of the presence of an inner doublet a combination of three peaks is observed. A singlet line is superimposed on the inner doublet. In $Ni_{0.3}Zn_{0.7}Fe_2O_4$ with 5% TiO_2 added, the relaxation spectrum shows only 5 peaks because the peaks have broadened to a large extent resulting in a single inner peak instead of inner doublet. When 10% TiO_2 is added the spectrum shows a relaxed six peak pattern in which the inner peaks are observed to be of narrower width than the outer ones.

A possible interpretation of the relaxed room temperature doublet may be sought in the domain wall theory of Srivastava *et al* (1976). However, Srivastava considers this effect as a comparatively smaller effect superimposed on the regular magnetic splitting. Since our experiments do not provide any information on the nature of the domain structure of our system, it was not possible to draw any conclusion about the nature of relaxation in our samples except that they are closer to the extreme case where the relaxation frequency is much larger than the Zeeman frequency.

The liquid nitrogen spectra clearly show that they fall in a region where neither of the extremities of the relaxation theory mentioned in the previous section is valid. However, certain important experimental results can be derived from our data. They are presented in tables 3 and 4.

Table 3 gives the Mössbauer hyperfine parameters measured at room temperature.

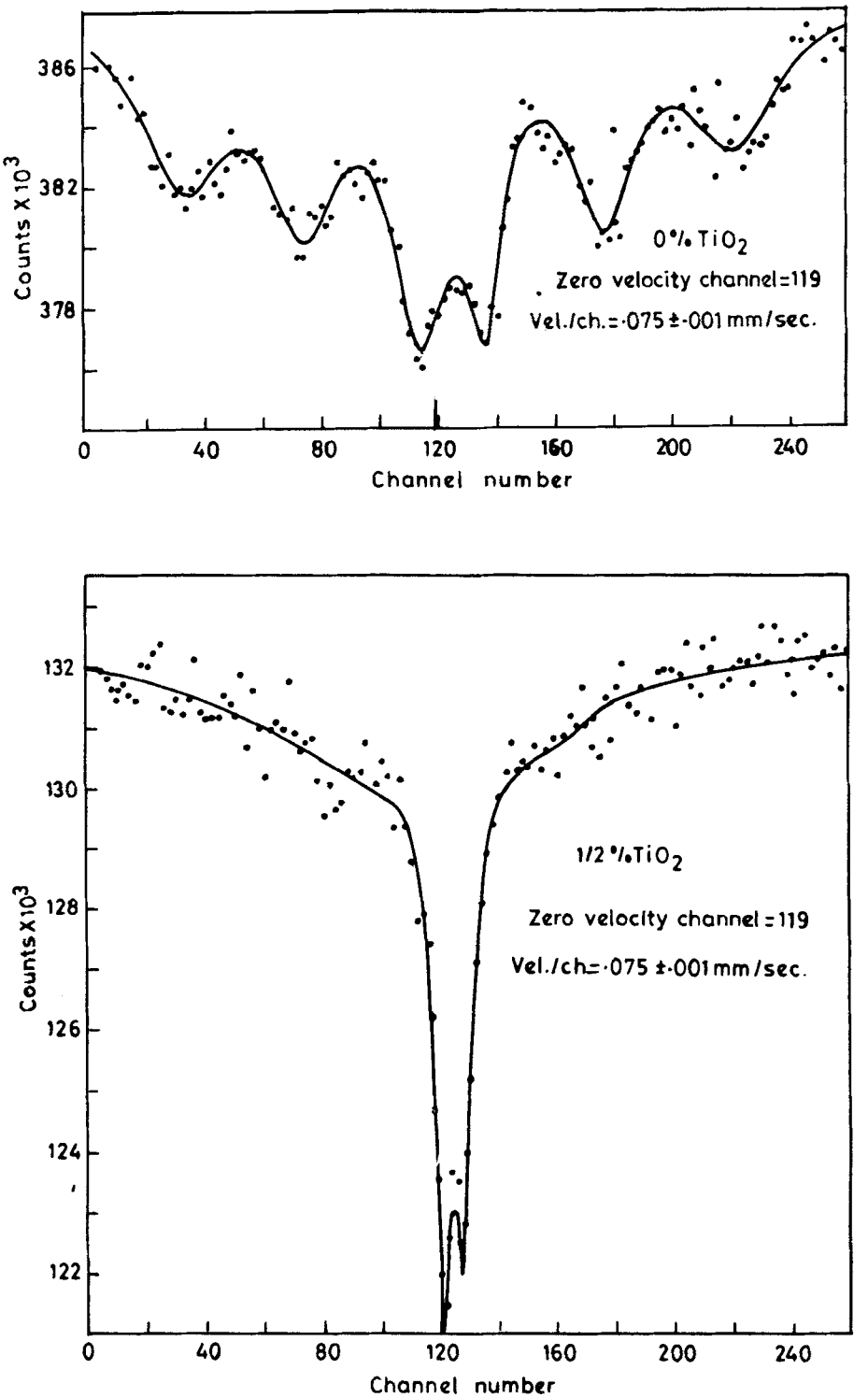

Figure 3. Room temperature Mössbauer spectra of $Ni_{0.3}Zn_{0.7}Fe_2O_4$ with 0 and 1/2 % TiO_2 addition.

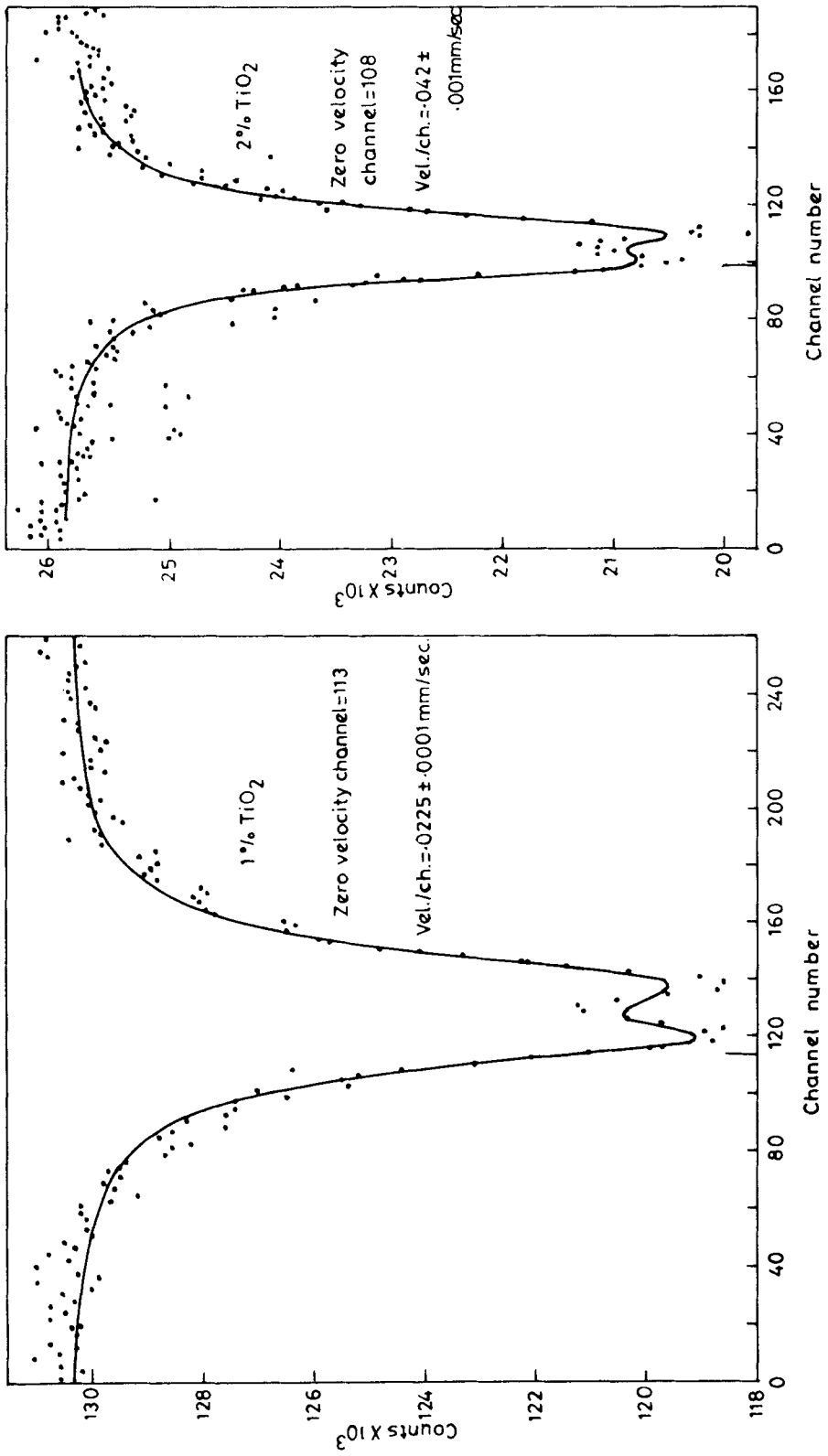

Figure 4. Room temperature Mössbauer spectra of $Ni_{0.3}Zn_{0.7}Fe_2O_4$ with 1 and 2% TiO_2 addition.

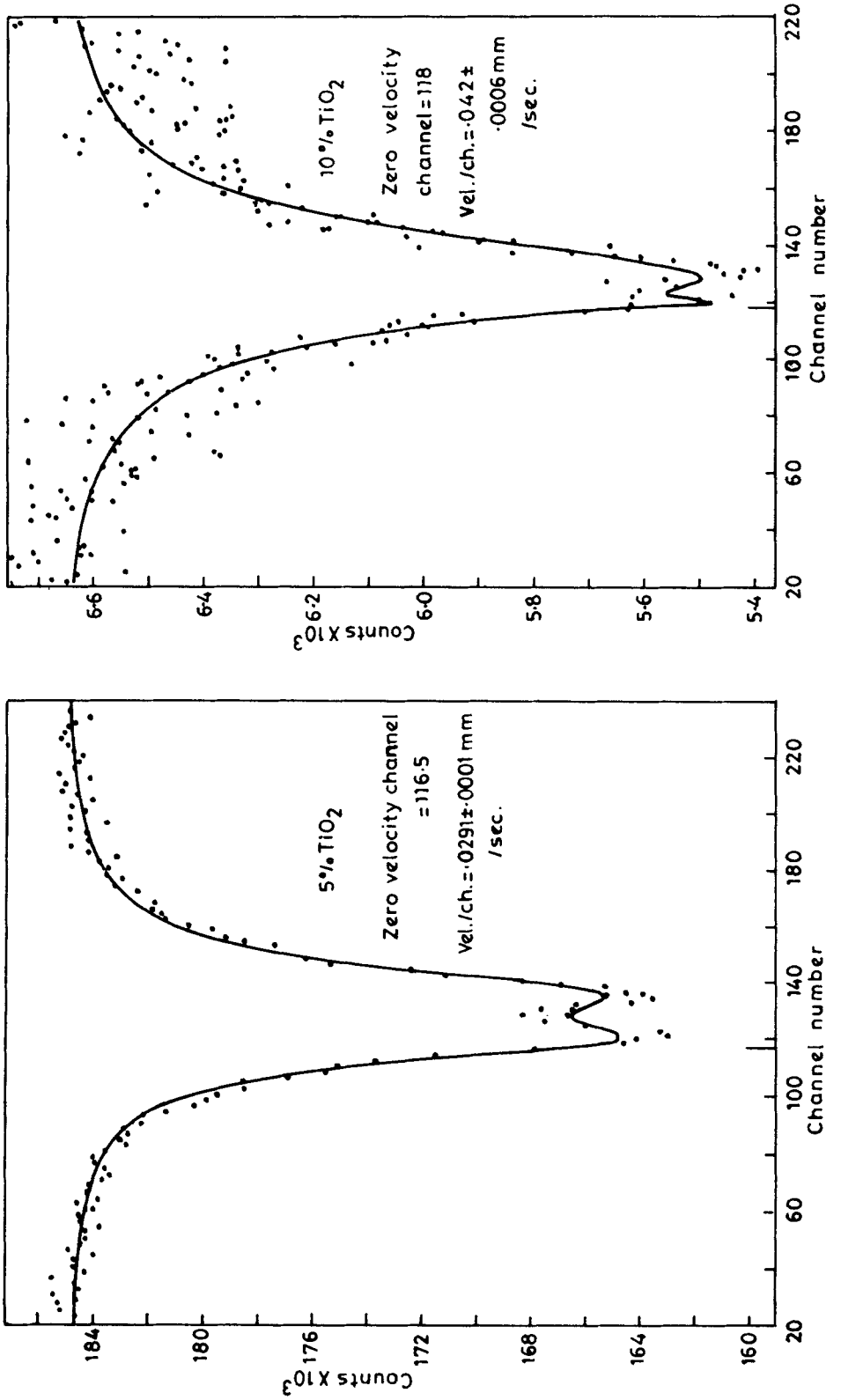

Figure 5. Room temperature Mössbauer spectra of $Ni_{0.3}Zn_{0.7}Fe_2O_4$ with 5 and 10% addition.

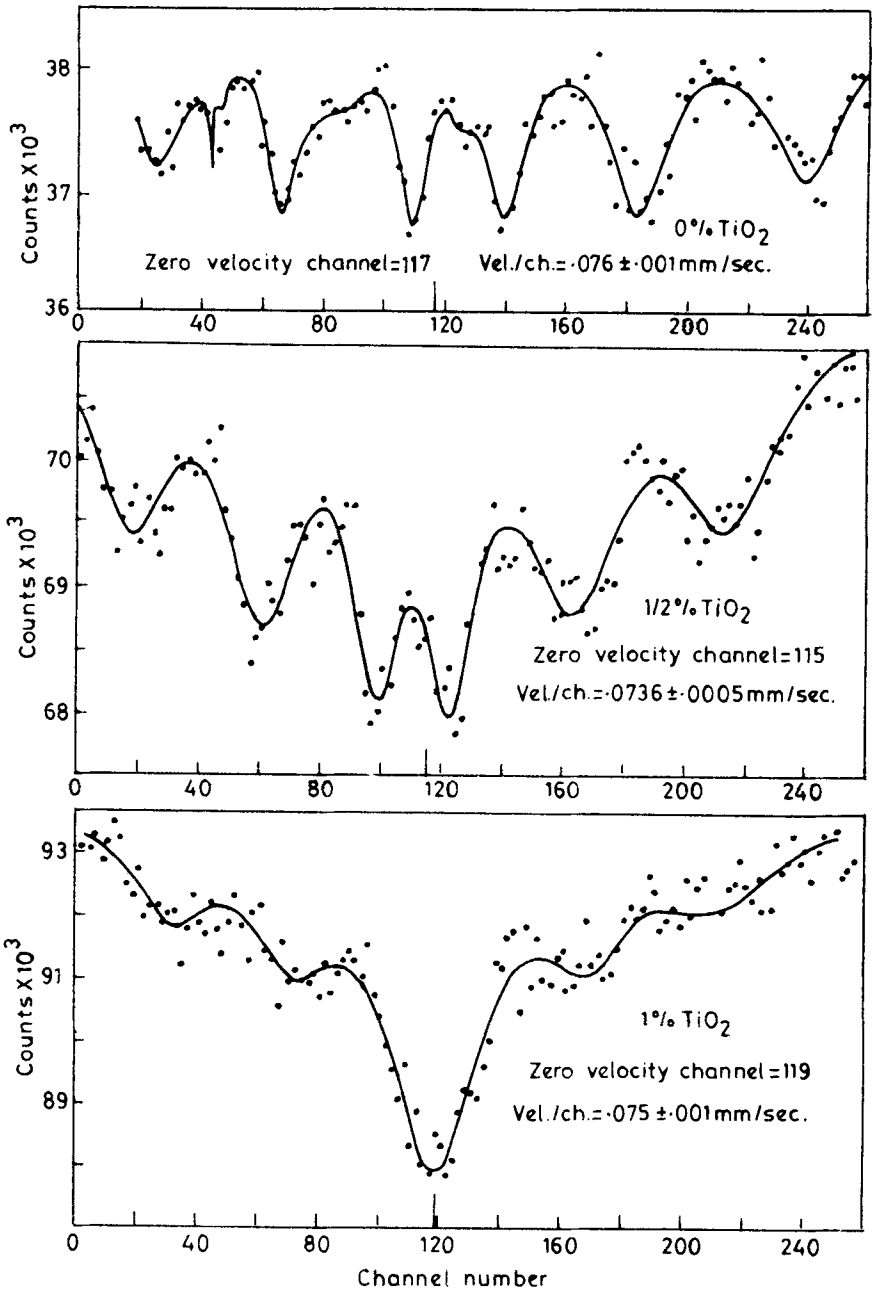

Figure 6. Mössbauer spectra of $Ni_{0.3}Zn_{0.7}Fe_2O_4$ with 0, 1/2 and 1 % TiO_2 addition at 77°K.

The isomer shift observed for the series is the order of 0·3 ± 0·05 mm/sec. The pure $Ni_{0.3}Zn_{0.7}Fe_2O_4$ sample which exhibits relaxed magnetic spectra gives almost zero quadrupole splitting; whereas in all other samples which exhibit paramagnetic spectra due to extreme relaxation the quadrupole splitting is of the order of 0·5 ± 0·02 mm/sec.

Table 4 gives the hyperfine parameters at liquid nitrogen temperature. All observed

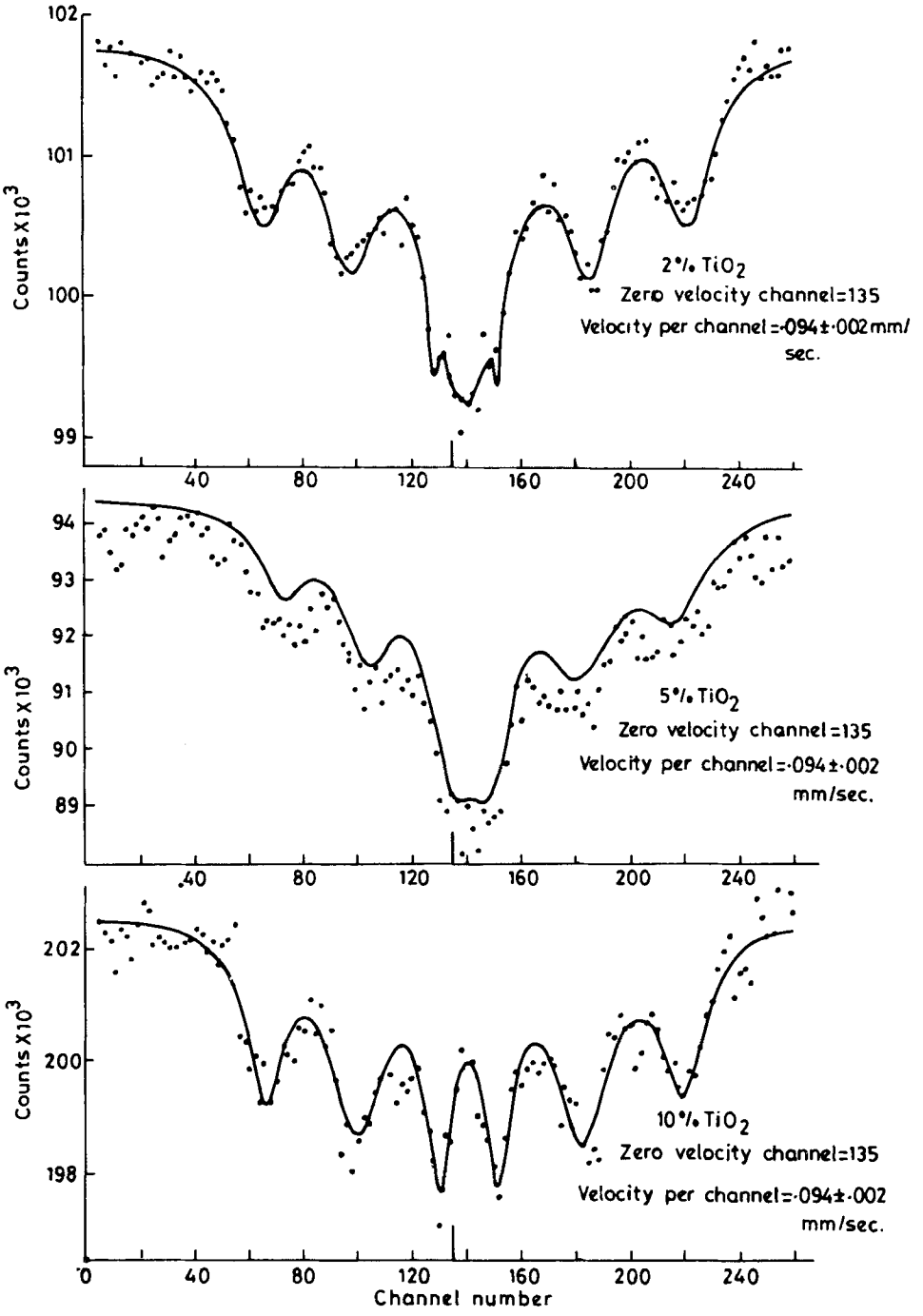

Figure 7. Mössbauer spectra of $Ni_{0\cdot3}Zn_{0\cdot7}Fe_2O_4$ with 2, 5 and 10% TiO_2 addition at 77°K.

spectra are Zeeman-split with various degrees of relaxation mechanism present. The average isomer shift is approximately 0·5 ± 0·05 mm/sec. Quadrupole splitting apparently decreases and the values of H_{eff} observed lie between 370 and 460 KOe.

Table 3. Mössbauer hyperfine parameters $Ni_{0.3}Zn_{0.7}Fe_2O_4$ with TiO_2 added at room temperature (300°K)

Weight percent of TiO_2 addition	Nature of observed spectrum	Isomer shift mm/sec	Quadrupole splitting (ΔE) mm/sec	H_{eff} KOe
0	Zeeman splitting (relaxed)	0·45 ± 0·05	0·15 ± 0·10	380 ± 20
1/2	Quadrupole split 2 peak spectra	0·38 ± 0·03	0·52 ± 0·02	—
1	-do-	0·35 ± 0·02	0·49 ± 0·02	—
2	-do-	0·26 ± 0·04	0·37 ± 0·05	—
5	-do-	0·33 ± 0·01	0·51 ± 0·02	—
10	-do-	0·24 ± 0·05	0·36 ± 0·05	—

Table 4. Mössbauer hyperfine parameters for $Ni_{0.3}Zn_{0.7}Fe_2O_4$ with TiO_2 addition at 77°K

TiO_2 addition Weight percent	Nature of observed spectrum	Isomer shift mm/sec	Quadrupole splitting (ΔE) mm/sec	H_{eff} KOe
0	Zeeman split (relaxed)	0·50 ± 0·06	0·50 ± 0·20	460 ± 20
1/2	-do-	0·40 ± 0·05	0·30 ± 0·10	390 ± 20
1	-do-	0·60 ± 0·10	0·12 ± 0·30	300 ± 25
2	-do-	0·50 ± 0·07	0·13 ± 0·10	450 ± 25
5	-do-	0·70 ± 0·20	0·20 ± 0·40	370 ± 50
10	-do-	—	0·13 ± 0·10	410 ± 25

The larger isomer shift observed at liquid nitrogen temperature is due to temperature difference between the source which is kept at room temperature and the absorber which is at liquid nitrogen temperature.

The values of isomer shift suggest that only Fe^{3+} ions are present in our samples and Fe^{2+} ions are not generated due to the addition of TiO_2 under oxidising atmosphere. The isomer shift observed for Fe^{2+} ions in ferrous oxide is 1·15 mm/sec, whereas our values are much smaller (~ 0·5 mm/sec.) which is more representative of Fe^{3+} ions (e.g. 0·47 for ferric oxide) (Kistner and Sunyar 1960).

We would like to comment that our interpretation in terms of relaxation are only qualitatively correct. There is no theory available for the relaxation in systems with vacancies. For a complete interpretation of our data an independent theoretical work in this direction is in order.

5. Resistivity measurements

Van Uitert (1955) studied the resistivity of Ni-Zn ferrite with slightly non-stoichiometric composition. He showed that a very little deficiency or excess of iron ions change the resistivity from a typically high value ($10^{10}\Omega$-cm) to a very low value

(~a few hundred Ω-cm). Baszynski (1969) found that the magnetic ordering in Ni-Zn ferrite lowers the generation of carriers whereas the mobility remains constant. Hence, activation energy obtained from the slope of the logarithm of resistivity vs. inverse temperature curve is higher in the ferrimagnetic region than in the paramagnetic region. Murthy and Sobnadri (1977) confirmed this and suggested that change in slope may be linked with magnetic ordering or may be due to a change in the conductivity mechanism.

The predominant conduction in Ni-Zn ferrite is due to the presence of Ni in octahedral sites which favors a conduction mechanism

$$Ni^{2+} + Fe^{3+} \rightleftharpoons Ni^{3+} + Fe^{2+} \tag{2}$$

again, the cation vacancies, if present, form the combination vacancy $-Fe^{3+}$ which act as a *p*-type acceptor and increase the resistivity. Stijntjes *et al* (1971) substituted $2Fe^{3+}$ ions by $Ti^{4+} + Fe^{2+}$ in a reducing atmosphere and found resistivity increase caused by the localization of Fe^{2+} ions near Ti^{4+} ions. Brabers (1976) found that the resistivity increases in Ti^{4+} substituted Mn and Zn ferrites due to (i) the formation of $Fe^{2+} - Ti^{4+}$ pairs lowering the site energy by about 0·03 eV and thus decreasing the electron mobility and (ii) the increased scattering of the electrons at higher Ti^{4+} concentrations.

For the present system, where Ti^{4+} is introduced under oxidizing atmosphere, the relative decrease of Ni^{2+} and Fe^{3+} will inhibit the mechanism given in (2) and thus increase the resistivity. Again, the process (ii) described in the last paragraph will still play a major role in the increase of resistivity.

6. Discussion

Table 5 shows the resistivity of the samples measured at room temperature. $Ni_{0.3}Zn_{0.7}Fe_2O_4$ shows a resistivity of about 400 ohms-cm. As soon as Ti^{4+} is added in the system, resistivity goes up by at least two orders of magnitude. For 1/2% TiO_2 addition the sample showed a resistivity as 6×10^4 ohms-cm at room temperature. Then for higher TiO_2 addition the resistivity changes between 10^4 ohms-cm to 10^5 ohms-cm. The variation of resistivity with TiO_2 addition is not very regular. For 2% TiO_2 addition it shows the maximum resistivity of $0{\cdot}8 \times 10^5$ ohms-cm.

Table 5. Measurement of resistivity at room temperature with different percentages of added TiO_2

Weight percentage of TiO_2 addition	Resistivity* (ohms-cm)
0	$0{\cdot}39 \times 10^3$
1/2	$60{\cdot}3 \times 10^3$
1	$36{\cdot}3 \times 10^3$
2	$85{\cdot}0 \times 10^3$
5	$63{\cdot}6 \times 10^3$
10	$12{\cdot}7 \times 10^3$

*Error in measurement ±1%.

Table 6 shows the temperature (T_a) at which change of slope is observed in log ρ vs. $1/T$ curve. For 0 and 1/2 % of TiO_2 added $Ni_{0.3}Zn_{0.7}Fe_2O_4$ samples, this temperature T_a is below the ferromagnetic transition temperature while for 1 % and higher TiO_2 addition T_a is observed to be above ferromagnetic transition temperature T_c. Tinsley (1980) has shown that this problem has still not reached a stage of clarification. He observed that T_a is lower than T_c for Fe_3O_4 and Ni substituted Fe_3O_4, while for Zn substituted Fe_3O_4, T_a and T_c are practically the same. We add to such observations by reporting T_a and T_c for TiO_2 substituted $Ni_{0.3}Zn_{0.7}Fe_2O_4$ series.

Table 7 gives the observed activation energies below and above the transition temperature T_a for samples with different amounts of added TiO_2. The average increase in activation energy is approximately 0·04 eV when the system becomes magnetically disordered. As soon as Ti^{4+} is added the activation energy increases. This increase is of the order of ~ 0·05 eV except for one sample i.e. the one with 2 % TiO_2 addition where it is approximately 0·1 eV.

7. Conclusion

A detailed theory of the Mössbauer relaxation spectra is outside the scope of the present work. But the work prepares the experimental background for an independent

Table 6. Temperature at which kink is observed in log ρ vs $1/T$ with different weight percentages of TiO_2 addition to $Ni_{0.3}Zn_{0.7}Fe_2O_4$

Weight percentage of TiO_2 addition	Temperature in °C	Ferromagnetic transition temperature in °C
0	150	196
1/2	97	104
1	144	81
2	135	113
5	122	101
10	112	77

Table 7. Energy gaps (ΔE) observed below and above resistivity kink temperature T_a for different percentages of TiO_2 addition to $Ni_{0.3}Zn_{0.7}Fe_2O_4$

Weight percentage of TiO_2 addition	ΔE_1 (eV)	ΔE_2 (eV)
0	0·21	0·17
1/2	0·25	0·22
1	0·25	0·23
2	0·31	0·26
5	0·28	0·25
10	0·24	0·21

theoretical work on Mössbauer relaxation phenomena for a complex system with vacancies. Finally we may state that further experiments with similar dopants (e.g. Zr^{4+}, Sn^{4+}, Nb^{5+} etc.) in the entire composition range ($x = 0{\cdot}0$ to $1{\cdot}0$) of $Ni_{1-x}Zn_xFe_2O_4$ is called for. The magnetization measurements, especially at low temperature, would improve our understanding of the vacancy distribution and the associated magnetic structure. The Mössbauer and the resistivity experiments would generate insight into the microscopic mechanisms essential for developing the appropriate generalised theories for Mössbauer relaxation and resistivity.

Acknowledgement

We are grateful to Prof. A R Das for growing the samples for us.

Appendix

The magnetic moments in the sublattices B_1 and B_2 are oriented at an angle $(\pi\text{-}\phi)$ in opposite directions with respect to the moments in the A sublattice. The canting angle is given by

$$M = M_B\cos\phi - M_A \tag{A1}$$

where M is the total magnetization, M_A is the magnetic moment of the A sublattice and $M_B\,(= 2M_{B1} = 2M_{B2})$ is the total magnetic moment of the B sublattice.

The effective fields acting on various ions are given by:

$$\begin{bmatrix} \bar{H}_A(\mathrm{Fe}) \\ \bar{H}_{B1}(\mathrm{Ni}) \\ \bar{H}_{B1}(\mathrm{Fe}) \\ \bar{H}_{B2}(\mathrm{Ni}) \\ \bar{H}_{B2}(\mathrm{Fe}) \end{bmatrix} = \begin{bmatrix} \lambda_{AA} & \alpha & \beta & \alpha & \beta \\ \alpha & \gamma & \varepsilon & \gamma & \varepsilon \\ \beta & \varepsilon & \delta & \varepsilon & \delta \\ \alpha & \gamma & \varepsilon & \gamma & \varepsilon \\ \beta & \varepsilon & \delta & \varepsilon & \delta \end{bmatrix} \begin{bmatrix} A\bar{m}_A(\mathrm{Fe}) \\ B_N\bar{m}_{B1}(\mathrm{Ni}) \\ B_F\bar{m}_{B1}(\mathrm{Fe}) \\ B_N\bar{m}_{B2}(\mathrm{Ni}) \\ B_F\bar{m}_{B2}(\mathrm{Fe}) \end{bmatrix} \tag{A2}$$

where $\bar{H}_A(\mathrm{Fe})$ is the effective molecular field acting on the Fe^{3+} ion at the A site due to all other ions etc. A, B_N, B_F are the concentrations of Fe^{3+}, Ni^{2+} and Fe^{3+} ions on A, B_1 or B_2 and B_1 or B_2 sublattices respectively. The molecular field coefficients α, β etc. represent the interactions $A(Fe^{3+})$-$B_1(Ni^{2+})$, $A(Fe^{3+})$-$B_1(Fe^{3+})$ etc. Also,

$$\begin{aligned} \bar{m}_i(\mathrm{Fe}) &= 5\mu_B, & i &= A,\ B1,\ B2 \\ \bar{m}_j(\mathrm{Ni}) &= 2{\cdot}3\mu_B, & j &= B1,\ B2 \\ \bar{m}_{Bi}\cdot\bar{m}_A &= -|\bar{m}_{Bi}|\ |\bar{m}_A|\cos\phi_{\mathrm{YK}}, & Bi &= B_1,\ B_2 \\ \bar{m}_{B1}\cdot\bar{m}_{B2} &= |\bar{m}_{B1}|\ |\bar{m}_{B2}|\cos 2\phi_{\mathrm{YK}}. \end{aligned} \tag{A3}$$

Minimizing the total magnetic interaction energy for the canting model the expression for Yafet-Kittel angle comes out to be

$$\cos\phi_{\mathrm{YK}} = \frac{23{\cdot}0\alpha AB_N + 50{\cdot}0\beta AB_F}{21{\cdot}16\gamma B_N^2 + 96{\cdot}0\varepsilon B_NB_F + 100{\cdot}0\delta B_F^2} \tag{A4}$$

The authors started with the exchange constant J values reported by Srivastava *et al* (1979) for the collinear region of $Ni_{1-x}Zn_xFe_2O_4$ and converted them to the molecular field constants using the relations

$$\lambda_{A-B} = (2Z_{AB} J_{A-B})/(N_B g_A g_B \mu_B^2) \tag{A5}$$

where Z_{AB} is the number of nearest neighbours of the B kind sorrounding the A kind, N_B is the number of B type ions per formula unit, g_A and g_B are the gyromagnetic ratios of the A and B ions respectively. These parameters were adjusted with the help of a computer program using (A4) to match with the reported angle (Satya Murthy *et al* 1969) for $Ni_{0.25}Zn_{0.75}Fe_2O_4$ and the angle for $Ni_{0.3}Zn_{0.7}Fe_2O_4$ obtained from our saturation moment data and (A1).

Using these parameters a computer program was written to adjust the transfer of iron from $A \rightleftharpoons B$ sites due to introduction of Ti^{4+}; this transfer is characterized by x'.

For a simplified description of the transfer process we break it up into three intermediate virtual processes:

(i) The addition of oxygen belonging to TiO_2 and the presence of Ti^{4+} with its charge conservation requirement generates 'vacancies' $\square_A$ and $\square_B$ as follows:

$$\begin{aligned}&(Zn_{0.7}Fe_{0.3})[Ni_{0.3}Fe_{1.7}]O_4 + xTiO_2 \Rightarrow \\ &(Zn_{0.7}Fe_{0.3})_{\left(\frac{4}{4+2x'}\right)} \square_{A\left(\frac{2x'}{4+2x'}\right)} [Ni_{0.15}Fe_{0.85}]_{2\left(\frac{4}{4+2x'}\right)} \\ &\square_{B\left(\frac{4x'}{4+2x'}\right)} Ti_{\left(\frac{4x'}{4+2x'}\right)} O_4\end{aligned} \tag{A6}$$

It is to be noted that the number of $\square_B$ sites is equal to the number of Ti^{4+} ions introduced and that of $\square_A$ sites is half the number of Ti^{4+} ions. Ti^{4+} are treated as non-magnetic ions and it is assumed that in slowly annealed samples, the Ni^{2+} ions remain in the octahedral sites and Zn^{2+} in tetrahedral sites.

(ii) We stipulate that the transfer of Fe^{3+} has to be only to a 'vacant' site. For a given sample we try to generate its experimental magnetic moment by a suitable number of transfers $m(A \rightarrow B)$ or $-m(B \rightarrow A)$. Writing m as a fraction

$$\begin{aligned}&m = x'({}^N\square_A) = x'({}^N\square_B)/2 = x'(N_{Ti^{4+}})/2 \\ &{}^N\square_A = (1+x')\,{}^N\square_A \\ &{}^N\square_B = \left(1 - \frac{x'}{2}\right){}^N\square_B \\ &-1 \leqslant x' \leqslant 2\end{aligned} \tag{A7}$$

(iii) Now,

$${}^N\square = {}^N\square_A + {}^N\square_B = {}^N\square'_A + {}^N\square'_B = \frac{3}{2} N_{Ti^{4+}}$$

where $N_{Ti^{4+}}$ is the number of Ti^{4+} ions.

Though as of now we have assumed the presence of Ti^{4+} ions we have not located them. We now put them in the 'vacancies' which would finally leave true vacancies equal to half the total number of Ti^{4+} ions, i.e. $\frac{1}{2}N_{Ti^{4+}}$. We now stipulate that this Ti^{4+} and the

true vacancy ratio is true not only for the entire crystal, but any of its subunits, leading to a homogeneous Ti^{4+} and true vacancy distribution. Hence the number of Ti^{4+} at A sites equal to $\frac{2}{3}{}^{N}\square'_{A}$ and the corresponding true vacancies are $\frac{1}{3}{}^{N}\square'_{A}$; similarly for the B sites.

So, finally, for a transfer represented by x' the formula can be written as

$$\begin{aligned}&\left(\mathrm{Zn}_{0.7\left(\frac{4}{4+2x}\right)}\,\mathrm{Fe}_{0.3\left\{\left(\frac{4}{4+2x}\right)-\frac{x'}{2}\left(\frac{4x}{4+2x}\right)\right\}}\right.\\&\left.\mathrm{Ti}_{\left(\frac{4x}{4+2x}\right)\left(\frac{1+x'}{2}\right)\cdot\frac{2}{3}}\,\square_{\left(\frac{4x}{4+2x}\right)\left(\frac{1+x'}{2}\right)\cdot\frac{1}{3}}\right)\\&\left[\mathrm{Ni}_{0.3\left(\frac{4}{4+2x}\right)}\,\mathrm{Fe}_{1.7\left\{\left(\frac{4}{4+2x}\right)+\frac{x'}{2}\left(\frac{4x}{4+2x}\right)\right\}}\right.\\&\left.\mathrm{Ti}_{\left(\frac{4x}{4+2x}\right)\left(\frac{2-x'}{2}\right)\cdot\frac{2}{3}}\,\square_{\left(\frac{4x}{4+2x}\right)\left(\frac{2-x'}{2}\right)\cdot\frac{1}{3}}\right]\mathrm{O}_4\end{aligned}\qquad\text{(A8)}$$

where x is the mole fraction of Ti^{4+} added.

For each value of x', the (A8) gives us the following: (i) M_B, (ii) M_A, (iii) A, B_N, B_F of (A4) and hence ϕ_{YK} and so, from (A1) (iv) the total magnetic moment M. The computer program iterates x' for the x values of the six samples and compares the results with the experimental magnetic moments till the agreement is reached. The entire process is repeated with the variations of the molecular parameters till we reach the best fit with the magnetic moment data.

References

Baszynski J 1969 *Acta Phys. Pol.* **35** 631

Blasse G 1964 *Philips Res. Rep. Suppl.* **3** 1

Blume M and Tjon J 1968 *Phys. Rev.* **165** 446

Bongers P F, van Groenou A B and Stuyts A L 1968 *Mater. Sci. Eng.* **3** 317

Brabers V A M 1976 *Appl. Phys.* **9** 347

Daniels J M and Rosencwaig A 1970 *Can. J. Phys.* **48** 381

Das A R, Ananthan V S and Khan D C 1985 *J. Appl. Phys.* **57** 4189

Dunitz J D and Orgel L E 1957 *J. Phys. Chem. Solids* **3** 318

Goldanskii V I and Belov V F 1965 *Zh. Eksp. Teor. Fiz.* **49** 1681

Goldanskii V I and Belov V F 1966 *Sov. Phys. JEPT (Engl. Transl.)* **22** 1149

Gorter E W 1954 *Philips Res. Rep.* **9** 295, 403

Khan D C, Misra M and Das A R 1982 *J. Appl. Phys.* **53** 2722

Kistner O C and Sunyar A W 1960 *Phys. Rev. Lett.* **4** 412

Leung L L, Evans B J and Morris A H 1973 *Phys. Rev.* **B8** 29

McClure D S 1957 *J. Phys. Chem. Solids* **3** 311

Murty V R K and Sobnadri J 1977 *Phys. Status Solidi* **A38** 647

Raj P, and Kulshrestha S K 1971 *Phys. Status Solidi* **A4** 501

Satya Murthy N S, Natera M G, Yussef S I, Begum R J and Srivastava C M 1969 *Phys. Rev.* **181** 969

Srivastava C M and Patni M J 1970 *J. Magn. Res.* **15** 359

Srivastava C M, Shringi S N and Srivastava R G 1976 *Phys. Rev.* **B14** 2041

Srivastava C M, Srinivasan G and Nandikar N G 1979 *Phys. Rev.* **B19** 499

Stijntjes T G W, Klerk J, Rooymans C J M, van Groenou A B, Pearson R F, Knowles J E and Rankin P 1970 *Ferrites, Proc. Int. Conf.* (Tokyo: Univ. Press) Vol. 191

Stijntjes T G W, Klerk J and van Groenou A B 1970 *Philips Res. Rep.* **25** 95

Tinsley C J 1980 *J. Magn. and Magn. Mater.* **15-18** 459

Van Uitert L G 1955 *J. Chem. Phys.* **23** 1883